JASA

ARTICLE

An impedance tube technique for estimating the insertion loss of earplugs

K. Carillo,[1,a)] O. Doutres,[1,b)] and F. Sgard[2,c)]

[1]*École de technologie supérieure (ÉTS), Montréal, Québec, Canada*

[2]*Institut de Recherche Robert-Sauvé en Santé et Sécurité du travail (IRSST), Montréal, Québec, Canada*

ABSTRACT:

This paper proposes a quick and straightforward technique for estimating the insertion loss (IL) of earplugs measured on an acoustical test fixture (ATF) using a commercial impedance tube. In this method, the earplug's acoustic properties (i.e., its transmission loss and the reflection coefficient of its medial surface) are determined from its transfer matrix measured using the three-microphones impedance tube method modified here for the current application. The IL is then estimated using a one-dimensional analytical model of open and occluded earcanals based on the wavefield decomposition theory. The method is evaluated numerically and experimentally from 50 Hz to 6.5 kHz. The numerical study allows for verifying the accuracy of the proposed approach in comparison to a simplified model of an ATF earcanal excited by normal incidence plane wave and diffuse field excitation. The experimental evaluation, which involves six earplugs (including five commercially available ones) representing various earplug families, demonstrates the accuracy of the estimation method, yielding results with a maximum difference of 3 dB compared to ATF measurements, on average, among the tested earplugs. © *2024 Acoustical Society of America.*

https://doi.org/10.1121/10.0028195

I. INTRODUCTION

Passive earplugs are commonly used as a last resort to prevent workers from noise-induced hearing loss (NIHL). Their performance is assessed through the sound attenuation that they provide, which can be quantified objectively through the insertion loss (IL) indicator. The IL corresponds to the differences in sound pressure levels (SPLs) measured in the open and occluded earcanals at the eardrum position for a given acoustic stimulation. One way to assess the IL provided by earplugs is to use an acoustical test fixture (ATF), according to standard ANSI/ASA S12.42.[1] ATFs include a synthetic human outer ear (i.e., pinna and earcanal that are partially covered by artificial skin) inserted into an artificial head and torso and terminated by a coupler that simulates the average acoustic impedance of the human middle ear. Compared to measurement on human subjects, the use of ATFs enables fast and repeatable measurements, making it particularly suitable for quality control, earplug design, and experiments in high noise level environments or impulsive sounds.

However, ATF measurements have three primary drawbacks: (i) ATFs typically use a single-size earcanal, assumed to represent an average human morphology, while variations in earcanal morphology among individuals can result in significant differences in personal attenuation rating provided by earplugs;[2] (ii) conducting ATF measurements requires cumbersome and costly experimental facilities, such as reverberant or anechoic chambers, to apply controlled acoustic conditions; and (iii) conducting earplug IL measurements on ATFs offers limited insights into the influence of intrinsic acoustic properties, such as acoustic reflection and transmission coefficients, on the phenomenon.

For a deeper understanding of earplugs inherent characteristics and their influence on the IL, Hiselius[3,4] introduced an alternative method that consists in measuring the acoustical two-port properties of the earplugs using a small impedance tube (9 mm inner diameter, similar to the adult earcanal) equipped with two sufficiently different termination impedances. Subsequently, the IL of the earplugs is determined by numerically connecting the two-port transfer matrix to an acoustic model of the earcanal, including the eardrum. This approach allows for estimating the IL of earplugs using a much simpler experimental setup than using an ATF. Moreover, the IL can be estimated for diverse earcanal geometries and various eardrum acoustic impedances corresponding to specific individuals. Predictions of the IL of several commercial earplugs were shown to approximately align with real ear attenuation at threshold (REAT) measurements performed on human subjects.[3,4] Although the method proposed by Hiselius is promising, using a small impedance tube poses certain technical challenges, including the incompatibility or need for relocation of standard 1/4 in. microphones, the necessity of a convergent setup when using a speaker larger than the tube's inner diameter, and

a)Email: kevin.carillo@etsmtl.ca
b)Email: olivier.doutres@etsmtl.ca
c)Email: franck.sgard@irsst.qc.ca

the significant influence of acoustic leakage. Furthermore, the two-port approach is not suitable for emphasizing the influence of key acoustic properties of the earplug (i.e., reflection coefficient of its medial surface and acoustic transmission) on the sound attenuation it provides.

More recently, following Hiselius' approach, Doutres et al.[5] introduced a comparable methodology for estimating the IL of earplugs measured on ATF. In this method, the calculation of the earplug's acoustic properties (i.e., transmission loss and reflection coefficient of the earplug medial surface) is performed according to the standard ASTM E2611-09 (Ref. 6) using a commercially available 29-mm inner-diameter impedance tube, overcoming technical challenges encountered by Hiselius using a small impedance tube.[3] Because the impedance tube is much larger than the earcanal, Doutres et al. used a sample holder that reproduces the earcanal geometry of an ATF, including the surrounding artificial skin, as it influences the acoustic behavior of earplugs through their boundary conditions. Then, the earplugs' acoustic properties are used as inputs to an analytical acoustic model of the earcanal to estimate the corresponding IL. The acoustic model of the earcanal is based on the wavefield decomposition theory and results in straightforward analytical relationships between the earplug and earcanal acoustic properties. Doutres et al. verified their method numerically using finite element (FE) models of the impedance tube setup and the ATF earcanal open and occluded by a silicone earplug. However, they assumed the earplug to be flush-mounted to the earcanal entrance and did not consider its protrusion outside the earcanal. Additionally, they did not perform an experimental evaluation of the proposed method.

In 2018, Carillo et al.[7] presented the initial results of an experimental evaluation of the method proposed by Doutres et al.[5] A major technical challenge encountered at that time using the three-microphones impedance tube method[8] was isolating the signal from the background noise at the microphone #3, located behind the sample holder, when the sound attenuation of the earplug became too significant. Consequently, experimental results became chaotic in certain frequency ranges, making the IL estimation method non-usable in practice. Impedance tube methods, typically based on standard ASTM E2611-09,[6] are generally employed for measuring key acoustic properties of air-saturated porous or fibrous media and not originally designed for assessing the acoustic properties of highly reflective and isolating systems such as earplugs. Additionally, a question arising from this work is whether the IL of earplugs depends on the excitation sound field. The impedance tube method provides earplug IL at normal incidence and, accordingly, the ATF measurements were also conducted that way. However, this approach may not be representative of the acoustic field experienced in practical usage. To investigate the influence of the excitation sound field on the earplug IL, Viallet et al.[9] conducted experimental measurements for normal incidence (in a semi-anechoic room) and diffuse field (in a reverberant room) excitations. They found "no significant differences" between the two conditions. However, the earplugs that they tested were flush-mounted to

the earcanal entrance and, therefore, the potential influence of the protrusion of earplugs outside the earcanal was not considered. Also, the pinna was also not accounted for (the earcanal was rather baffled) despite its potential influence on the IL, depending on the characteristics of the excitation sound field.

The aim of this paper is to enhance the method introduced by Doutres et al.,[5] providing an experimental impedance tube approach capable of accurately estimating the IL of earplugs measured on ATFs. This method offers practical advantages: (i) It eliminates the need for a cumbersome acoustic room by using a commercial impedance tube, (ii) facilitates the incorporation of earcanal geometry variability by using different cost-effective sample holders, and (iii) allows for the direct inclusion of eardrum impedance inter-variability in a post-processing step.

Here, the modified impedance tube method for assessing the IL of earplugs is evaluated numerically and experimentally. The numerical evaluation involves two earplugs, one representing a "custom-molded" silicone earplug and another representing a "roll-down foam" with a notable protrusion outside the entrance of the earcanal. A simplified approach for incorporating the acoustic effect of the protrusion is presented here. Additionally, the numerical study explores the influence of the sound pressure field (normal incidence plane wave versus diffuse field) on the earplugs' IL. The experimental evaluation involves six earplugs, where five of them are commercially available and represent various earplug families. The experimental evaluation aims at predicting the earplugs' IL measured on a G.R.A.S. 45CB (G.R.A.S. Sound and Vibration SA, Holte, Denmark, Denmark) ATF using the impedance tube technique. This ATF is chosen because it provides a convenient test bench with a cylindrical earcanal that is easy to reproduce in the impedance tube setup. Additionally, this ATF is known to comply with the ANSI/ASA S12.42 standard.[10] In this paper, we also address the technical challenge of improving the signal-to-noise ratio at microphone #3 of the impedance tube by decreasing the radius of its downstream section, and the corresponding equations of the impedance tube method are modified accordingly.

This paper is structured as follows. In Sec. II, we detail the analytical model of the IL, depending on the acoustic properties of the earplug and earcanal. We also present the procedure for determining the earplug acoustic properties from the modified impedance tube setup. Furthermore, we describe the experimental setups of the ATF and impedance tube measurements and their corresponding FE models to evaluate the proposed method numerically and experimentally. In Sec. III, we present the numerical and experimental results and discuss the accuracy of the proposed method for estimating the IL of earplugs. In Sec. IV, we conclude this paper and provide perspectives.

II. METHODOLOGY

A. Analytical model of the IL

Figure 1 displays schematics of the open [Fig. 1(a)] and occluded [Fig. 1(b)] earcanals. The earcanal is cylindrical, of length l_{EC} and radius r_{EC}, and corresponds to the earcanal
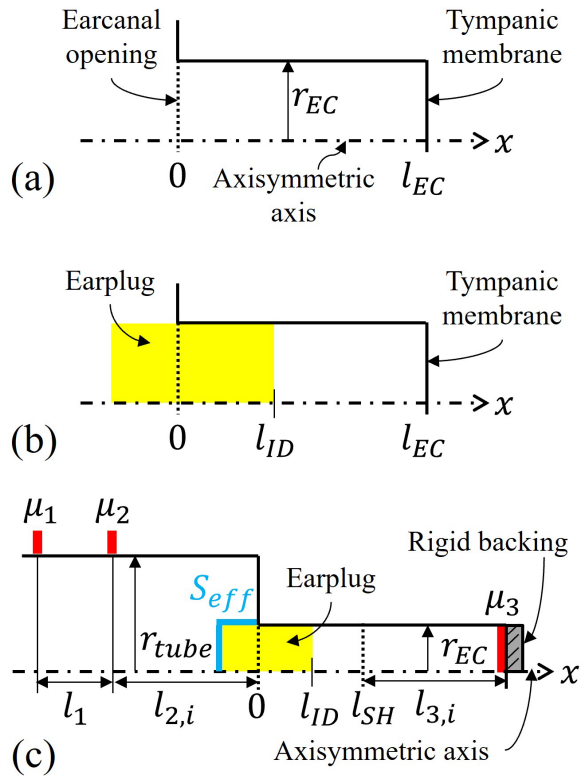
FIG. 1. (Color online) Schematic representation of the (a) open and (b) occluded earcanals of the ATF setup along with (c) the impedance tube setup is displayed.

of the ATF used for the experimental evaluation of the proposed method (see the experimental setup in Sec. II C 1). For the purpose of evaluating the proposed method for estimating the IL, the pinna is not accounted for, yet, to simplify the problem. Hence, the earcanal entrance is rather considered to be flush-mounted onto a rigid baffle. In the occluded case, the insertion depth of the earplug from the earcanal entrance is denoted by l_{ID}.

The acoustic pressure field in open and occluded earcanals is described using the wavefield decomposition theory under the assumption of one-dimensional (1D) plane wave propagation along x axis. The temporal dependency is taken as $e^{j\omega t}$, where j is the imaginary unit, ω is the circular frequency, and t is the time. In open and occluded cases, a normal incident plane wave of amplitude P_0 impinges on the baffled earcanal at $x = 0$. Although the viscothermal effects have little influence (less than 0.5 dB) on the acoustic pressure within open and occluded earcanal cavities, they are accounted for in this study for the sake of precision. This is achieved by employing an equivalent complex wavenumber, denoted by k_{eq}^{EC}, and computed using a low reduced frequency model[11] (see Appendix B). The acoustic radiation at the earcanal opening ($x = 0$) is accounted for by the acoustic radiation impedance, Z_R, of a baffled circular piston[12] (see Appendix A). At the eardrum ($x = l_{EC}$), the equivalent acoustic impedance, Z_{TM}, of a coupler mimicking the eardrum acoustic impedance in the experimental setup is used.[9] Note that specific acoustic impedances (i.e., pressure to

normal particle velocity ratio), Z_R and Z_{TM}, are introduced in the analytical model through their corresponding reflection coefficients, R_R and R_{TM}, respectively, defined such that

$$R_i = \frac{Z_i - Z_{eq}^{EC}}{Z_i + Z_{eq}^{EC}}, \quad i \in \{R, TM\}, \tag{1}$$

where Z_{eq}^{EC} represents the equivalent characteristic impedance of the air in the earcanal, incorporating viscothermal effects (see Appendix B). In the occluded case, the acoustic behavior of the earplug is accounted for through (i) its sound transmission coefficient, τ_{EP}, from the surrounding environment to the earcanal cavity, and (ii) the reflection coefficient, R_{EP}, of its medial surface ($x = l_{ID}$), observed from the earcanal cavity.

Taking into account the multiple wave reflections in the open earcanal through forward (x-direction) and backward ($-x$-direction) plane waves, the total sound pressure field at a given position, x, gives[13]

$$p_{open}(x) = \frac{A_{open}\left(e^{-jk_{eq}^{EC}x} + R_{TM}e^{-2jk_{eq}^{EC}l_{EC}}e^{jk_{eq}^{EC}x}\right)}{1 - R_R R_{TM}e^{-2jk_{eq}^{EC}l_{EC}}}, \quad 0 \le x \le l_{EC}, \tag{2}$$

where $A_{open} = 2P_0 Z_{eq}^{EC}/(Z_R + Z_{eq}^{EC})$ represents the amplitude of the acoustic wave entering the open earcanal, accounting for the incident, reflected, and radiated pressures at $x = 0$.

In the occluded case, we assume that the lateral surface of the earplug is located at $x = 0$ regardless of the earplug length. In the general case, where the earplug has a protrusion outside the earcanal ($x < 0$), the acoustic effect of the protrusion is accounted for when determining the acoustic properties of the earplug (see the details in Sec. II B). The acoustic pressure field in the occluded earcanal is obtained in a similar way to that in the open earcanal with three exceptions: (i) The amplitude of the acoustic wave entering the occluded earcanal cavity through the earplug at $x = l_{ID}$ is equal to $A_{occl} = \tau_{EP}P_0$, where τ_{EP} is the transmission coefficient of the earplug in a semi-infinite space; (ii) backward plane waves ($-x$-direction) now face the medial surface of the earplug backed by a semi-infinite space and characterized by the reflection coefficient, R_{EP}, defined at $x = l_{ID}$; and (iii) the total length of the occluded earcanal is equal to $l_{EC} - l_{ID}$. Hence, based on Eq. (2), the acoustic pressure at a given position, x, of the occluded earcanal writes

$$p_{occl}(x) = \frac{A_{occl}\left(e^{-jk_{eq}^{EC}x} + R_{TM}e^{-2jk_{eq}^{EC}l_{EC}}e^{jk_{eq}^{EC}x}\right)}{1 - R_{EP}R_{TM}e^{-2jk_{eq}^{EC}(l_{EC}-l_{ID})}}, \quad l_{ID} \le x \le l_{EC}. \tag{3}$$

From Eqs. (2) and (3), the IL of the earplug is calculated as the difference in SPLs at the eardrum ($x = l_{EC}$) between open and occluded cases and can be decomposed such that

$$IL = TL_{EP} + IL_c, \tag{4}$$

where TL_{EP} is the transmission loss of the earplug and IL_c is a factor that depends on the characteristics of the open and occluded earcanals,

$$TL_{EP} = 20 \log_{10}\left(\frac{1}{|\tau_{EP}|}\right), \quad (5)$$

$$IL_c = 20 \log_{10}\left(\frac{2\left|Z_{eq}^{EC}\right|}{\left|Z_R + Z_{eq}^{EC}\right|} \times \frac{\left|1 - R_{EP}R_{TM}e^{-2jk_{eq}^{EC}(l_{EC}-l_{ID})}\right|}{\left|1 - R_R R_{TM} e^{-2jk_{eq}^{EC}l_{EC}}\right|}\right). \quad (6)$$

It is noteworthy to mention that the same modelling approach can be used (see Ref. 5) to provide a straightforward analytical relation of the noise reduction (NR), which is equal to the difference between the IL and transfer function of the open ear (TFOE).[14]

B. Determination of the earplug acoustic properties

In the proposed method, the acoustic properties of the earplug (i.e., R_{EP} and τ_{EP}) are determined at normal incidence using a three-microphones impedance tube method,[8] based on the standard ASTM E2611-09,[6] and modified here specifically for the current application. The modification is detailed below and involves using a downstream section (including microphone #3) that is much thinner than the upstream section (including microphones #1 and #2) of the commercial impedance tube setup used in this work.

Under the assumption of plane wave propagation in x-direction, the transfer matrix, $\mathbf{T}_{EP}$, of the earplug relates the acoustic pressure, p, and the normal particle velocity, v, from $x = 0$ to $x = l_{ID}$ such that

$$\begin{bmatrix} p \\ v \end{bmatrix}_{x=0} = \mathbf{T}_{EP} \begin{bmatrix} p \\ v \end{bmatrix}_{x=l_{ID}} = \begin{bmatrix} T_{11}^{EP} & T_{12}^{EP} \\ T_{21}^{EP} & T_{22}^{EP} \end{bmatrix} \begin{bmatrix} p \\ v \end{bmatrix}_{x=l_{ID}}. \quad (7)$$

The reflection coefficient, R_{EP}, of the earplug medial surface observed from the earcanal cavity corresponds to the ratio between reflected and backward ($-x$-direction) incident pressures at $x = l_{ID}$. The transmission coefficient, τ_{EP}, of the earplug from the external environment to the earcanal cavity rather corresponds to the ratio between transmitted and forward (x-direction) incident pressures at $x = 0$. From the earplug transfer matrix, $\mathbf{T}_{EP}$, the acoustic coefficients, R_{EP}, and τ_{EP} are calculated by

$$R_{EP} = \frac{T_{11}^{EP} + T_{12}^{EP}/Z_{eq}^{EC} - T_{21}^{EP}Z_{eq}^{EC} - T_{22}^{EP}}{T_{11}^{EP} + T_{12}^{EP}/Z_{eq}^{EC} + T_{21}^{EP}Z_{eq}^{EC} + T_{22}^{EP}}, \quad (8)$$

$$\tau_{EP} = \frac{2e^{jk_{eq}^{EC}l_{ID}}}{T_{11}^{EP} + T_{12}^{EP}/Z_{eq}^{EC} + T_{21}^{EP}Z_{eq}^{EC} + T_{22}^{EP}}. \quad (9)$$

In the proposed method, the earplug is inserted in a sample holder that mimics the cylindrical earcanal of the ATF. The length of the sample holder is denoted by l_{SH} [see Fig. 1(c)]. In this setup, the insertion depth of the earplug should not exceed the length of the sample holder (i.e., $l_{ID} \leq l_{SH}$). The transfer matrix of the sample holder is referred to as $\mathbf{T}_{EP,SH}$ and includes the earplug and a portion of the earcanal cavity. From $\mathbf{T}_{EP,SH}$, the transfer matrix of the earplug is obtained as

$$\mathbf{T}_{EP} = \mathbf{T}_{EP,SH}\mathbf{T}_{cav}^{-1}, \quad (10)$$

where $\mathbf{T}_{cav}$ accounts for the portion of the sample holder that is not filled with the earplug but rather with air and defined by

$$\mathbf{T}_{cav} = \begin{bmatrix} \cos\left(k_{eq}^{EC}l_{cav}\right) & jZ_{eq}^{EC}\sin\left(k_{eq}^{EC}l_{cav}\right) \\ \dfrac{-1}{jZ_{eq}^{EC}}\sin\left(k_{eq}^{EC}l_{cav}\right) & \cos\left(k_{eq}^{EC}l_{cav}\right) \end{bmatrix}, \quad (11)$$

where $l_{cav} = l_{SH} - l_{ID}$. Note that the earplug IL can be estimated even in the case where l_{ID} is not known. It simply requires calculating $R_{EP,SH}$ and $\tau_{EP,SH}$ of the sample holder (including the earplug and a portion of earcanal cavity filled with air) from $\mathbf{T}_{EP,SH}$ using Eqs. (8) and (9). Then, in Eqs. (5) and (6) of the earplug IL estimation, $R_{EP,SH}$ and $\tau_{EP,SH}$ are introduced instead of R_{EP} and τ_{EP}, and l_{ID} is replaced by l_{SH}.

In the general case, the earplug inserted in the sample holder is not a symmetrical system (i.e., $T_{11}^{EP} \neq T_{22}^{EP}$). Therefore, the impedance tube method requires the use of two acoustic loads, $\{a, b\}$. According to Eq. (22) of standard ASTM E2611-09,[6] the transfer matrix, $\mathbf{T}_{EP,SH}$, of the sample holder (including the earplug) in terms of acoustic pressure and particle velocity on both sides (at $x = 0$ and $x = l_{SH}$) is given by

$$\mathbf{T}_{EP,SH} = \frac{1}{p_a(l_{SH})v_b(l_{SH}) - p_b(l_{SH})v_a(l_{SH})} \begin{bmatrix} p_a(0)v_b(l_{SH}) - p_b(0)v_a(l_{SH}) & p_b(0)p_a(l_{SH}) - p_a(0)p_b(l_{SH}) \\ v_a(0)v_b(l_{SH}) - v_b(0)v_a(l_{SH}) & p_a(l_{SH})v_b(0) - p_b(l_{SH})v_a(0) \end{bmatrix}. \quad (12)$$

The determination of pressures, p_i, and velocities, v_i, $i \in \{a, b\}$, in Eq. (12) depends on the geometrical configuration of the impedance tube. The impedance tube used experimentally (setup detailed in Sec. II C 2) includes three microphones:[8] microphones #1 and #2 are upstream of the sample to be measured, and microphone #3 is downstream,

as depicted in Fig. 1(c) and, respectively, referred to as μ_1, μ_2, and μ_3. Microphone #3 is flush-mounted on a hard termination. The upstream section of the impedance tube has an inner radius denoted by r_{tube}. The sample holder fits in the impedance tube and has an inner radius that is equal to the earcanal radius, r_{EC}, which is smaller than r_{tube}. The

downstream section of the impedance tube between the sample holder and microphone #3 has the same inner radius, r_{EC}, as the sample holder. This allows for an increase in the SPL at microphone #3 compared to the case in which the downstream section has the radius of the impedance tube. This resolves the technical challenge mentioned in the Introduction and related to improving the signal-to-noise ratio at microphone #3, which is located behind the sample holder, when the sound attenuation of the earplug became too significant. Based on Eq. (6) of Ref. 8 and dedicated to the three-microphones impedance tube method, pressures and velocities for the two different loads, $i \in \{a, b\}$, are given by

$$p_i(0) = -2e^{jk_{eq}^{tube}l_{2,i}}$$

$$\times \frac{H_{12,i}\sin\left(k_{eq}^{tube}(l_1 + l_{2,i})\right) - \sin\left(k_{eq}^{tube}l_{2,i}\right)}{H_{12,i}e^{-jk_{eq}^{tube}l_1} - 1},$$

$$v_i(0) = \frac{1}{Z_{eq}^{tube}} 2e^{jk_{eq}^{tube}l_{2,i}}$$

$$\times \frac{H_{12,i}\cos\left(k_{eq}^{tube}(l_1 + l_{2,i})\right) - \cos\left(k_{eq}^{tube}l_{2,i}\right)}{H_{12,i}e^{-jk_{eq}^{tube}l_1} - 1}$$

$$\times \frac{S_{tube}}{S_{eff}},$$

$$p_i(l_{SH}) = -2e^{jk_{eq}^{tube}l_{2,i}} \frac{H_{13,i}\sin\left(k_{eq}^{tube}l_1\right)\cos\left(k_{eq}^{EC}l_{3,i}\right)}{H_{12,i}e^{-jk_{eq}^{tube}l_1} - 1},$$

$$v_i(l_{SH}) = \frac{1}{Z_{eq}^{tube}} 2e^{jk_{eq}^{tube}l_{2,i}} \frac{H_{13,i}\sin\left(k_{eq}^{tube}l_1\right)\sin\left(k_{eq}^{EC}l_{3,i}\right)}{H_{12,i}e^{-jk_{eq}^{tube}l_1} - 1}.$$

$$(13)$$

Compared to Ref. 8, the expression of the velocities, $v_i(0)$, in Eq. (13) is modified to account for the change in section between the impedance tube upstream section and the sample holder at $x = 0$, where the continuity of volume flow is applied. This change in section is accounted for by the ratio, S_{tube}/S_{eff}, where $S_{tube} = \pi r_{tube}^2$ is the cross section of the impedance tube upstream section, and S_{eff}, in the general case, is the total surface area of the portion of the earplug that protrudes outside the sample holder [see Fig. 1(c)]. This approach enables the incorporation of the earplug's protrusion effects directly in its transfer matrix, from which the earplug acoustic properties are derived and subsequently used in the analytical model of the IL (see Sec. II A). When the earplug is flush-mounted in the sample holder earcanal, S_{eff} is equal to S_{EC}.[5]

In Eq. (13), k_{eq}^{tube} and Z_{eq}^{tube} are, respectively, the equivalent complex wavenumber and characteristic impedance accounting for viscothermal effects in the impedance tube upstream section using a low reduced frequency model[11] while k_{eq}^{EC} and Z_{eq}^{EC} are their counterparts in the downstream section. $H_{12,i} = p_i(\mu_2)/p_i(\mu_1)$ and $H_{13,i} = p_i(\mu_3)/p_i(\mu_1)$ are the acoustic pressure transfer functions between microphones #1 and #2 and microphones #1 and #3 of the

impedance tube. Lengths l_1, $l_{2,i}$, and $l_{3,i}$ correspond, respectively, to the distances between (i) microphones #1 and #2, (ii) microphone #2 and the sample holder ($x = 0$), and (iii) the sample holder ($x = l_{SH}$) and microphone #3. Note that $l_{2,a}$ and $l_{2,b}$ are generally taken to be equal. The two different acoustic loads required by the impedance tube method correspond to different lengths of $l_{3,i}$, $i \in \{a, b\}$. To avoid a singularity in the determination of $\mathbf{T}_{EP}$, the condition $l_{3,b} - l_{3,a} < 172/f_u$ must be fulfilled,[8] where f_u is the upper frequency limit of the impedance tube in Hz (detailed in Sec. II C 2). Finally, $S_{tube} = \pi r_{tube}^2$ is the cross section of the impedance tube upstream section, and S_{eff} is the total surface area of the portion of the earplug that protrudes outside the sample holder [see Fig. 1(c)]. In a simplified way, the ratio, S_{tube}/S_{eff}, in the expression of the velocities, $v_i(0)$ [see Eq. (13)], accounts for the change in section between the impedance tube upstream section and the earplug protrusion at the entrance of the sample holder ($x = 0$) where the continuity of volume flow is applied.

C. Experimental setups

1. Artificial test fixture measurement

As mentioned in the Introduction, the IL measurements are performed using a commercial ATF (G.R.A.S. 45CB, G.R.A.S. Sound and Vibration SA), depicted in Figs. 2(a) and 2(b), based on ANSI/ASA S12.42–2010.[1] The heating system included in the ATF to simulate the body temperature is turned off as it cannot be accounted for yet in the impedance tube measurement. The ear simulator (G.R.A.S. 40AG) is composed of a cylindrical earcanal partially covered by a 10 mm long silicon layer (of thickness 1.7 mm) from the earcanal entrance [see Fig. 2(c)]. The earcanal is terminated by a coupler (IEC 60318-4, G.R.A.S. Sound and Vibration SA) simulating the middle ear impedance according to the standard ANSI/ASA S3.25–2009.[15] As mentioned previously, the pinna is not included in this work but rather replaced by a metal plate flush-mounted around the earcanal entrance [see Fig. 2(b)]. Although the proposed method for estimating the IL is designed for normal incidence plane wave stimulation (see Secs. II A and II B), numerical simulations (detailed in Sec. II D 1) will illustrate that the IL does not undergo significant changes under diffuse field stimulation (results presented in Sec. III A), at least in the absence of the pinna, in agreement with study by Viallet et al.[9] As a result, ATF experimental measurements are conducted in a diffuse sound field generated by four loudspeakers (type JAMO® S628, Klipsch Group, Inc., Glyngøre, Denmark) within a reverberant room. This approach is preferred because of its ease of generation and it is more representative of the complex sound fields encountered in workplaces compared to normal incidence plane wave excitation. Using the microphone included in the coupler of the artificial test fixture, SPLs are measured in open and occluded earcanals, respectively, denoted by L_p^{open} and L_p^{occl}, to calculate the IL using

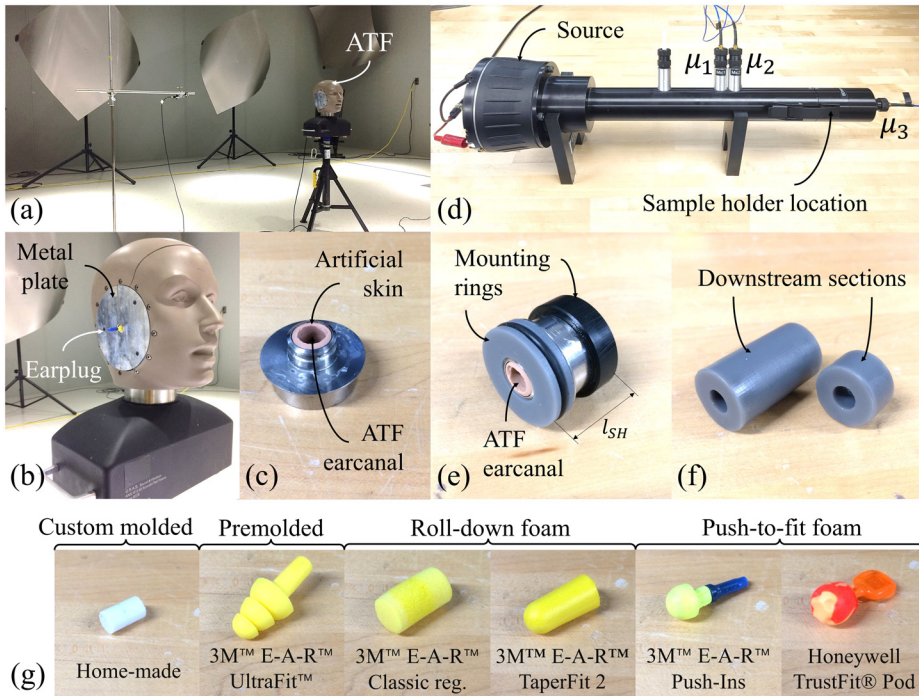$$IL = L_p^{open} - L_p^{occl}. \qquad (14)$$

FIG. 2. (Color online) (a) ATF placed in the reverberant room, (b) zoomed-in view of the ATF, (c) ATF earcanal, (d) impedance tube experimental setup, (e) sample holder of the impedance tube, (f) downstream sections of the impedance tube for the two acoustic loads, and (g) tested earplugs are shown.

2. Impedance tube measurement

In this work, a commercial impedance tube (Mecanum, Sherbrooke, Canada), as shown in Fig. 2(d), is employed to characterize the transfer matrix of the earplug, following the standard ASTM E2611-09 (Ref. 6) and Ref. 8. However, as we modified the impedance tube method to account for (i) the effect of the earplug protrusion outside the earcanal and (ii) the use of a "small" downstream section with the radius of the earcanal rather than the impedance tube radius (see Sec. II B), a portion of the post-processing performed separately using a MATLAB routine (MATLAB 2023a, MathWorks, Inc., Natick, MA).

The impedance tube upstream section has a radius $r_{tube} = 14.5$ mm. Hence, the upper frequency limit, defined by $f_u < Kc/2r_{tube}$, where $K = 0.586$ and $c \approx 345$ m/s is the sound speed in the tube, ensures plane wave propagation up to approximately 6.5 kHz. The impedance tube includes three $\frac{1}{4}$ in. microphones (MPA416, BSWA, Beijing, China). The two measured transfer functions, $H_{12,i}$ and $H_{13,i}$, where $i \in \{a, b\}$, are corrected (amplitude and phase correction) following the sensor-switching technique detailed in ASTM E2611-09.[6] The output signal is a white noise generated by a 4 in. loudspeaker. The sample holder is made of the ATF earcanal and two acoustically rigid plastic mounting rings [see Fig. 2(e)]. One of the mounting rings is flush-mounted to the earcanal entrance to correspond to the ATF experimental setup. By using the ATF earcanal in the sample holder of the impedance tube setup, a tested earplug can be inserted only once for both measurement techniques, ensuring that the boundary conditions of the earplug are kept identical between impedance tube and ATF measurements for comparison purposes. The total length of the sample holder is equal to $l_{SH} = 23.6$ mm [see the sample holder in Fig. 2(e)].

The distance between microphones #1 and #2 is equal to $l_1 = 20$ mm to cover the frequency range 200 Hz–6.5 kHz. For measurements below this frequency range, $l_1 = 100$ mm was used. Due to the geometric configuration of the experimental setup, the distance between microphone #2 and the sample holder takes different values for the two acoustic loadings such that $l_{2,a} = 114.3$ mm and $l_{2,b} = 89.6$ mm. Finally, the distances between the sample holder and microphone #3 (i.e., the downstream sections) are equal to $l_{3,a} = 11.25$ mm and $l_{3,b} = 35.96$ mm for the two acoustic loads. The two downstream sections, depicted in Fig. 2(f), are not part of the commercial impedance tube setup and were three-dimensionally printed using the stereo-lithography technique (Form 2 printer, Formlabs, Sommerville, MA). Post-cure, the mechanical properties of the resin (Grey pro V1, Formlabs; 2.6 GPa Young's modulus and 1200 kg/m³ density) ensure that the three-dimensionally printed structures are acoustically rigid.

3. Tested earplugs and the measurement procedure

The proposed method for estimating the IL is evaluated for various earplugs, including one homemade earplug and five commercial disposable earplugs from two different manufacturers, all of which are depicted in Fig. 2(g). These encompass one earplug from the "custom-molded" family, one multi-flange earplug from the "premolded" family, two earplugs from the "roll-down-foam" family, and two earplugs from the "push-to-fit foam" family. The custom-molded silicone earplug is cylindrical with a length of 14 mm and radius of 8 mm. The insertion depth was only measured for the silicone earplug and is equal to 6 mm. For the other earplugs, the insertion depth was not precisely measured and approximately ranges between 6 and 12 mm.

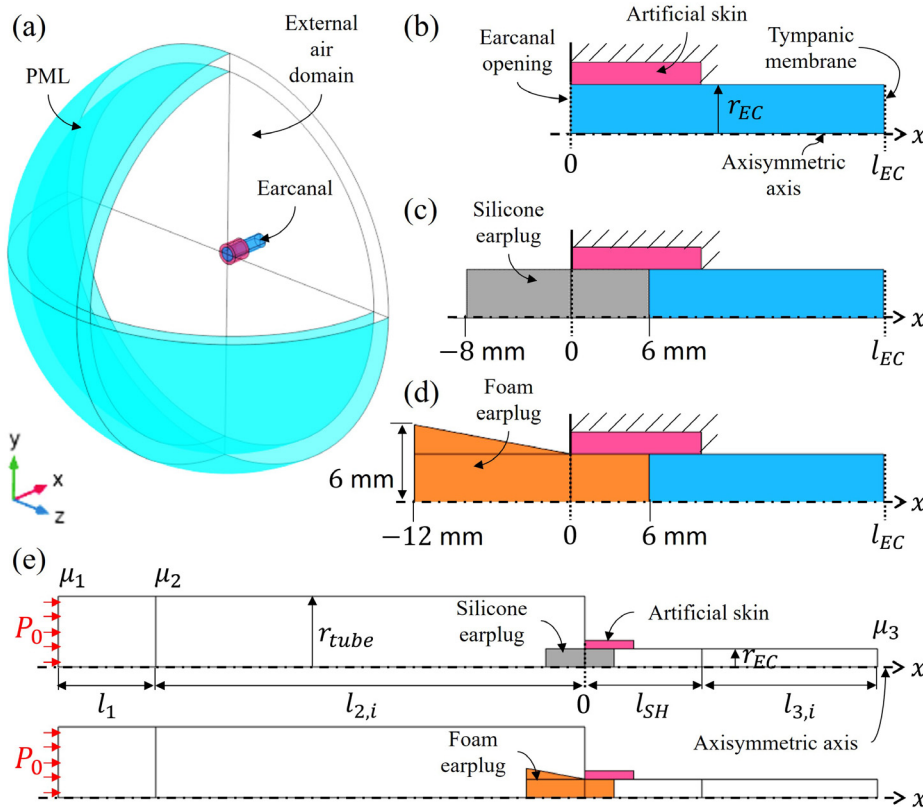J. Acoust. Soc. Am. **156** (2), August 2024

Carillo *et al.*   903

FIG. 3. (Color online) Schematics of the FE models, showing (a) 3D FE model of the ATF open earcanal, including the external air domain surrounded by the perfectly matched layer (PML), (b)–(d) 2D axisymmetric view of the ATF earcanal open and occluded by the silicone and foam earplugs, and (e) 2D axisymmetric FE model of the impedance tube setup.

For each earplug, ATF and impedance tube measurements were successively performed without removing the earplug from the artificial earcanal such that the boundary conditions and insertion depth of the earplug remain the same between the two methods.

D. Numerical models

In this work, we developed numerical models of the ATF setup and impedance tube setup based on the FE method using COMSOL Multiphysics® 6.1 (Stockholm, Sweden) to verify the analytical approach presented in Secs. II A and II B for estimating the IL of any earplug.

1. Artificial test fixture

Figure 3(a) displays the three-dimensional (3D) FE model of the open earcanal, corresponding to the ATF earcanal surrounded by air, as used in the experimental setup presented in Sec. II C 1. Note that the scattering effect of the ATF is neglected, and the earcanal is assumed to be embedded in a flat infinite rigid baffle.[9] The earcanal consists of a cylindrical duct partially surrounded with artificial skin layer [see Fig. 3(b)]. Figures 3(c) and 3(d) display the two-dimensional (2D) axisymmetrical views of the occluded earcanal for two distinct earplugs: one silicone earplug from the custom-molded family and one foam earplug from the roll-down-foam family. Both earplugs are inserted at 6 mm from the earcanal entrance. These two earplugs were chosen because they exhibit very different shape and material properties, effectively representing the range of earplugs tested experimentally (see Sec. II C 3).

The air in the external domain, as well as in the open and occluded earcanal cavities, is modeled as a compressible fluid. Viscothermal losses that occur in the earcanal are accounted for using the low reduced frequency model[11] (see Appendix B). The artificial skin layer and earplugs are modeled as linear isotropic elastic solid domains. Their material properties are taken from the literature and summarized in Table I.

In open and occluded cases, the equivalent acoustic impedance, Z_{TM}, of the coupler is defined at the eardrum surface of the earcanal. Also, the external air domain is surrounded by a perfectly matched layer (PML)[16] [see Fig. 1(a) for the open configuration], which simulates the Sommerfeld radiation condition at infinity (no reflection). Furthermore, the artificial skin is fixed on its circumferential and medial surfaces. Also, the wall of the portion of the earcanal cavity that is not coupled with the artificial skin is acoustically rigid.

Regarding the excitation, the diffuse sound field generated in the experimental setup (see Sec. II C 1) is modeled as a combination of uncorrelated freely propagating plane

TABLE I. Material properties of the artificial skin layer (Ref. 9), the silicone earplug (Ref. 17), and the foam earplug (Ref. 20). Young's modulus, E_s; density, ρ_s; Poisson's ratio, ν_s; structural loss factor, η_s.

	E_s (MPa)	ρ_s (kg m^{-3})	ν_s (1)	η_s (1)
Artificial skin	0.42	1050	0.43	0.2
Silicone earplug	2.9	1500	0.49	0.2
Foam earplug	0.1	220	0.1	0.5

904   J. Acoust. Soc. Am. 156 (2), August 2024

Carillo et al.

waves,[17] each with equal amplitude, $P_0 = 1$ Pa, and different directions. Each incident plane wave, characterized by the elevation angle, $\theta \in [0, \pi/2]$, and azimuthal angle, $\varphi \in [0, 2\pi]$, in the (y, z) plane [refer to Fig. 3(a)], can be expressed as

$$p(\theta, \varphi) = P_0 \exp[-j(k_x x + k_y y + k_z z)], \qquad (15)$$

where $k_x = k_0\cos(\theta)$, $k_y = k_0\sin(\theta)\cos(\varphi)$, $k_z = k_0\sin(\theta) \times \sin(\varphi)$, and $k_0 = \omega/c_0$ is the free field wavenumber.

In open and occluded configurations, the mean square acoustic pressure, $\left|p_{TM}^d\right|^2$, induced by the diffuse sound field at the eardrum is given by

$$\left|p_{TM}^d\right|^2 = \int_0^{2\pi} \int_0^{\pi/2} \left|p_{TM(\theta, \varphi)}\right|^2 \sin(\theta)\, d\theta\, d\varphi, \qquad (16)$$

where $p_{TM(\theta, \varphi)}$ is the acoustic pressure computed at the eardrum for a given plane wave incidence. As the system's geometry is axisymmetric around the x axis, the acoustic pressure at the eardrum is independent of the azimuthal angle, φ, leading to

$$\left|p_{TM}^d\right|^2 = 2\pi \int_0^{\pi/2} \left|p_{TM(\theta)}\right|^2 \sin(\theta)\, d\theta. \qquad (17)$$

The 3D FE model displayed in Fig. 3(a) is, thus, reduced to an axisymmetric problem, which is efficiently calculated using a four-points Gauss integration scheme[18] in open and occluded configurations.

As mentioned previously (refer to the Introduction and Sec. II C 1), in this work, we examine the potential influence of the acoustic excitation field on the simulated IL through numerical testing. For this purpose, an excitation by a normal incidence plane wave with an amplitude $P_0 = 1$ Pa is also employed instead of the diffuse sound field.

In all FE models, the continuity of stress vectors and displacements is assumed at the interfaces between solid domains. At fluid–structure interfaces, the continuity of normal component velocity vectors and normal component stress vectors applies. For more details on the FE formulations, the reader is referred to Ref. 19. The geometry is meshed according to a criterion of at least six elements per wavelength at 6.5 kHz (maximum frequency of interest) to achieve convergence. In 3D models, ten-noded (quadratic) tetrahedral elements are employed, whereas six-noded (quadratic) triangular elements are used in 2D axisymmetric models. In solid domains, the shortest wavelength between compression waves and shear waves is taken for calculating the mesh criteria. Sound speeds associated with longitudinal and shear waves are, respectively, defined in three dimensions by $c_L = \sqrt{E_s(1 - \nu_s)/[\rho_s(1 + \nu_s)(1 - 2\nu_s)]}$ and $c_S = \sqrt{E_s/[2\rho_s(1 + \nu_s)]}$. Regarding the PML domain, 12-noded (quadratic) prismatic elements are employed in 3D models, whereas 8-noded (quadratic) quadrangular elements are used in 2D axisymmetric models.

2. Impedance tube

Figure 3(e) displays the 2D axisymmetric FE model of the impedance tube corresponding to the experimental apparatus presented in Sec. II C 2. Impedance tube dimensions, r_{tube}, r_{EC}, l_1, $l_{2,i}$, $l_{3,i}$, where $i \in \{a, b\}$, and l_{SH} are given in Sec. II C 2. In the model, a unit pressure amplitude, $P_0 = 1$ Pa, is applied on the cross section corresponding to microphone #1 location to simulate the normal incidence excitation. The impedance tube boundaries are considered to be acoustically rigid. Material properties of the artificial skin and earplugs, as well as FE formulations and mesh criteria, are the same as those for the ATF FE model (see Sec. II D 1). Also, the determination of the acoustic properties of the earplugs from the impedance tube setup is described in Secs. II C 2 and II B.

III. RESULTS AND DISCUSSIONS

A. Numerical evaluation

We start by investigating numerically the accuracy of the modified impedance tube method designed for estimating the IL of earplugs. In particular, our goal is to assess the effectiveness of the method for earplugs with a significant protrusion [see Figs. 3(c) and 3(d)], given that the original method was initially assessed exclusively with a flush-mounted earplug.[5] Additionally, as mentioned in the Introduction, we investigate whether the IL provided by earplugs is influenced by the incident sound pressure field, namely, whether it is a normal incidence plane wave or diffuse field. For these purposes, Fig. 4 displays the IL of the silicone [Fig. 4(a)] and the foam [Fig. 4(b)] earplugs calculated using the ATF FE model for normal incidence plane wave and diffuse field excitations and also estimated using the FE model associated with the impedance tube technique. Numerical results are presented in narrowband from 50 Hz to 6.5 kHz with a frequency step of 5 Hz. Note the inverse orientation of the y axis, where the IL is displayed from the highest (bottom) to the lowest (top) value, as usual in the hearing protection field.

According to Figs. 4(a) and 4(b), the IL estimated by the impedance tube method (blue dashed lines) is nearly identical to the IL simulated on the ATF under normal incidence plane wave excitation (red lines with square markers) for silicone and foam earplugs. The averaged deviation is about 0.15 dB for the silicone earplug (with a maximum deviation of 1 dB at 6.5 kHz) and 0.4 dB for the foam earplug (with a maximum of 1.4 dB around 1.1 kHz). Thus, the impedance tube method, previously verified numerically in the case of a flush-mounted silicone earplug,[5] is also numerically verified here in the case of realistic earplugs protruding outside the earcanal. However, as the impedance tube technique relies on plane wave propagation and is typically applied to samples with flat surfaces on both sides, one might question how protrusions affect the acoustic field. To address this, Fig. 4(c) illustrates the acoustic pressure and velocity fields in the impedance tube at various frequencies
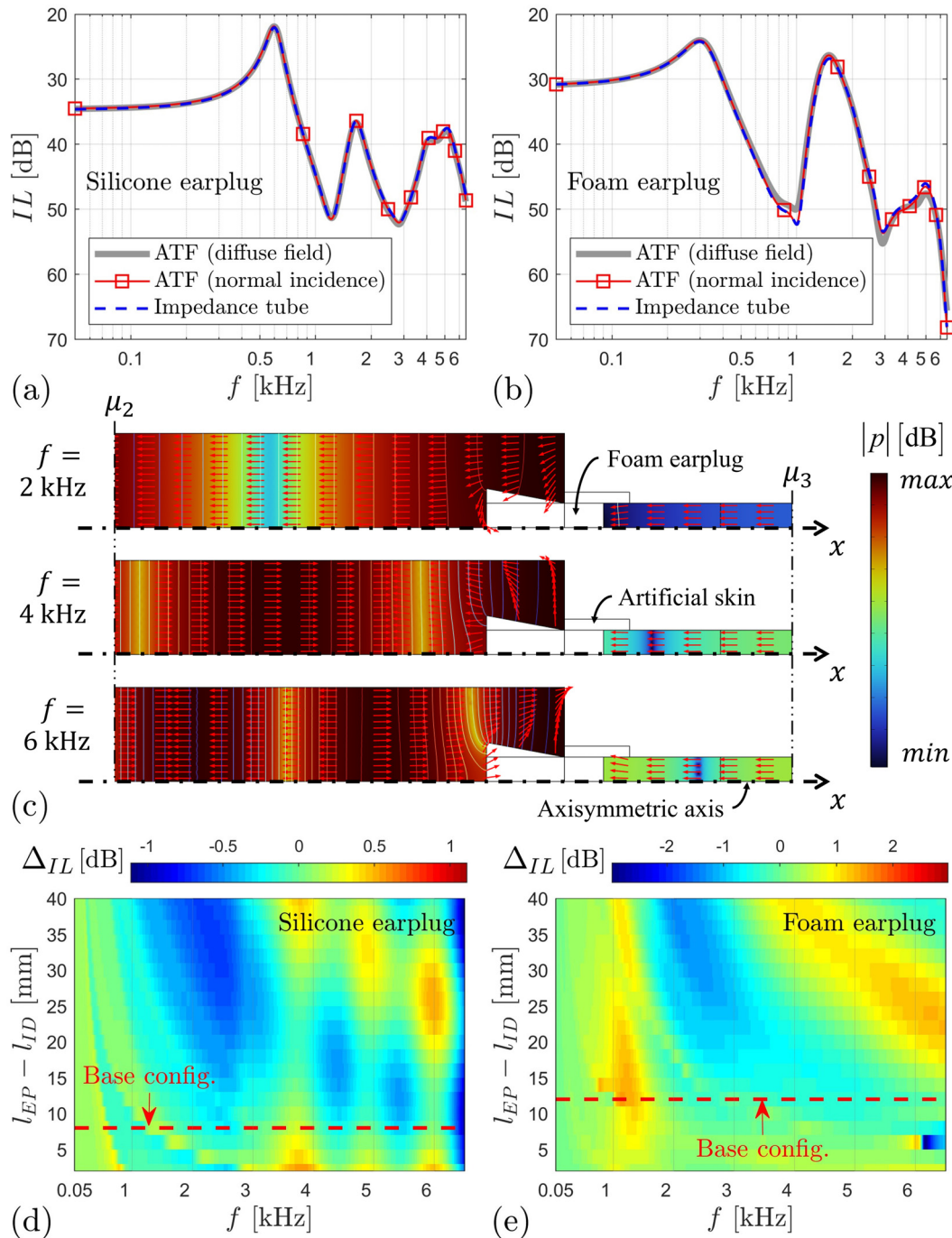
FIG. 4. (Color online) Numerical simulation of the IL provided by (a) the silicone earplug and (b) the foam earplug using ATF and impedance tube method, and (c) acoustic pressure (colormap) and velocity (red arrows, normalized) fields in the impedance tube at different frequencies for the foam earplug (base configuration) are shown. Frequency-dependent difference (ΔIL) in IL between the impedance tube method and ATF under normal incidence plane wave excitation is depicted as a function of the protrusion length ($l_{EP} - l_{ID}$), where l_{EP} is the total length of the earplug, for (d) silicone and (e) foam earplugs. In both cases, l_{ID} remains equal to 6 mm while l_{EP} is increased from 8 to 46 mm.

for the foam earplug, which has the largest protrusion. As the frequency increases, plane wave propagation is increasingly disrupted in the vicinity of the earplug because of acoustic wavelengths approaching the size of the protrusion. Nevertheless, the acoustic field in the upstream section becomes progressively more plane-like as the distance from the earplug increases. Positioning microphone #2 at a distance of at least two tube diameters[6] ensures a plane

acoustic field at the microphone's location, which is critical for accurate impedance tube measurements.

To investigate whether the robustness of the impedance tube method is influenced by the length of the earplug protrusion, Figs. 4(d) and 4(e) show the frequency-dependent difference (ΔIL) in IL between the impedance tube method and ATF under normal incidence plane wave excitation as a function of the protrusion length ($l_{EP} - l_{ID}$), where l_{EP} is the

total length of the earplug, for silicone and foam earplugs. In both cases, l_{ID} remains equal to 6 mm while l_{EP} is increased from 8 to 46 mm. For the silicone earplug [see Fig. 4(d)], ΔIL does not exceed approximately ± 1 dB, even for protrusion lengths up to 40 mm. For the foam earplug [see Fig. 4(e)], ΔIL does not exceed about ± 1.5 dB, on average, with a maximum deviation of -2.9 dB around 6 kHz for $l_{EP} - l_{ID} = 6$ mm, due to a slight frequency shift (not shown here) of an antiresonance between the two methods. These results provide a verification of the simplified approach detailed in Sec. II B to account for the acoustic effect of the protrusion through the continuity of the volume flow at the earcanal entrance [see the term S_{tube}/S_{eff} in the expression of $v_i(0)$ in Eq. (14)]. Similar to Figs. 4(d) and 4(e), Figs. 9(a) and 9(b) in Appendix C display the frequency-dependent difference (ΔIL) in IL between the impedance tube and ATF (normal incidence plane wave excitation), but S_{eff} is assumed to be equal to S_{EC} in the impedance tube method, thereby disregarding the protrusion effect. Although this has little impact on silicone earplugs (the maximum deviation does not exceed ± 1.5 dB), for foam earplugs, the maximum deviation can exceed 10 dB. This discrepancy arises because silicone earplugs, which are much stiffer as a result of their higher Young's modulus (see Table I), exhibit significantly lower velocities, $v_i(0)$ (not depicted here), compared to foam earplugs. Consequently, $v_i(0)$ plays a more important role in determining the acoustic properties of foam earplugs than that for silicone earplugs. Hence, the effective surface, S_{eff}, involved in the expression of $v_i(0)$ has a more pronounced effect in the case of foam earplugs than that for silicone earplugs.

Returning to Figs. 4(a) and 4(b), we observe that the simulated IL on the ATF under normal incidence plane wave and diffuse sound field yields very similar results for both earplugs. The average deviation is about 0.4 dB for the silicone earplug (with a maximum deviation of 0.7 dB around 6 kHz) and 0.8 dB for the foam earplug (with a maximum of 2.6 dB at 2.9 kHz). The larger deviation in the case of the foam earplug is primarily a result of the greater size of its protrusion compared to that for the silicone earplug used in this study. Indeed, as the size of the protrusion increases, the acoustic pressure gradient induced by the normal incidence plane wave around the earplug deviates more significantly from the uniform diffuse sound field, thus, modifying the vibro-acoustic behavior of the earplug. Nevertheless, the difference in IL between the two sound pressure fields remains very acceptable. Therefore, although the method for estimating the earplug IL from impedance tube measurements is theoretically designed for normal incidence excitation, it provides an IL as representative as that obtained for a more realistic acoustic field, at least when the pinna is not considered.

B. Experimental evaluation

Following the numerical evaluation, we now investigate experimentally the impedance tube technique for estimating

the IL of earplugs measured on the G.R.A.S. 45CB (G.R.A.S. Sound and Vibration SA) ATF that was described in Sec. II C 1. The goal is to compare the two methods without altering the insertion conditions of a given earplug. For this purpose, Fig. 5 displays the IL of six different earplugs (see their characteristics detailed in Sec. II C 3) measured on the ATF and estimated using the proposed impedance tube technique. The self-IL of the ATF measured using the closed earcanal made of steel is also displayed. Experimental results are presented in the third octave band between 63 Hz and 5 kHz and calculated from narrowband results using a MATLAB routine (MATLAB 2023a, MathWorks, Inc., Natick, MA) based on the ANSI S1.11 standard.[21] Note that at the "transition frequency," the impedance tube data shift from the large microphonic space between microphones #1 and #2 (i.e., $l_1 = 100$ mm) to the small microphonic space between microphones #1 and #2 (i.e., $l_1 = 20$ mm) to cover the entire frequency range of interest.

According to Fig. 5, the impedance tube method provides good estimates of the IL measured on the ATF for all six tested earplugs across the entire frequency range. In particular, the IL estimates effectively capture the frequency-dependent variations of the ILs measured on the ATF, which are notably different among the tested earplugs. At the transition frequency (i.e., 250 Hz), we can observe that the two microphonic spaces used in the impedance tube setup yield similar estimates of the IL. At the transition frequency, the averaged difference among the tested earplugs is about 0.1 dB while the largest difference is approximately 1 dB [see Fig. 5(f)]. Figure 6 displays the difference (mean $\pm$ standard deviation), denoted Δ_{IL}, between the third octave band ILs measured on ATF and estimated using the proposed impedance tube method for the six tested earplugs. On average, across frequencies, the absolute value of the IL difference between ATF and impedance tube methods is approximately 0.8 dB. The maximum deviation between the two methods is around 3.5 dB and occurs in the frequency band centered at 1.25 kHz. In this frequency band, as evident from Fig. 5, there is a notable decrease in the self-IL of the ATF used in this study. Consequently, the IL measured on the ATF can be underestimated as a substantial amount of energy may transfer through the structure of the ATF to the occluded earcanal. At low frequencies (below 0.1 kHz), the small self-IL of the ATF that we used (see Fig. 5) is also deemed to be a contributing factor to the 1–2 dB discrepancies observed between the impedance tube method and ATF (see Fig. 6). According to the standard,[1] the ATF must exhibit a minimum self-IL of 60 dB from 80 Hz to 12.5 kHz. Our ATF does not meet the standard below 0.4 kHz and in the third octave band centered at 1.25 kHz because of unidentified parasitic structural sound transfer pathways. On the contrary, the impedance tube method can easily circumvent this issue.

The 1D analytical model of the earcanal, on which the impedance tube method is based, enables the decomposition of the IL into two terms, TL_{EP} and IL_c, associated with the acoustic properties of the earplug [see Eq. (4) in Sec. II A].

J. Acoust. Soc. Am. **156** (2), August 2024
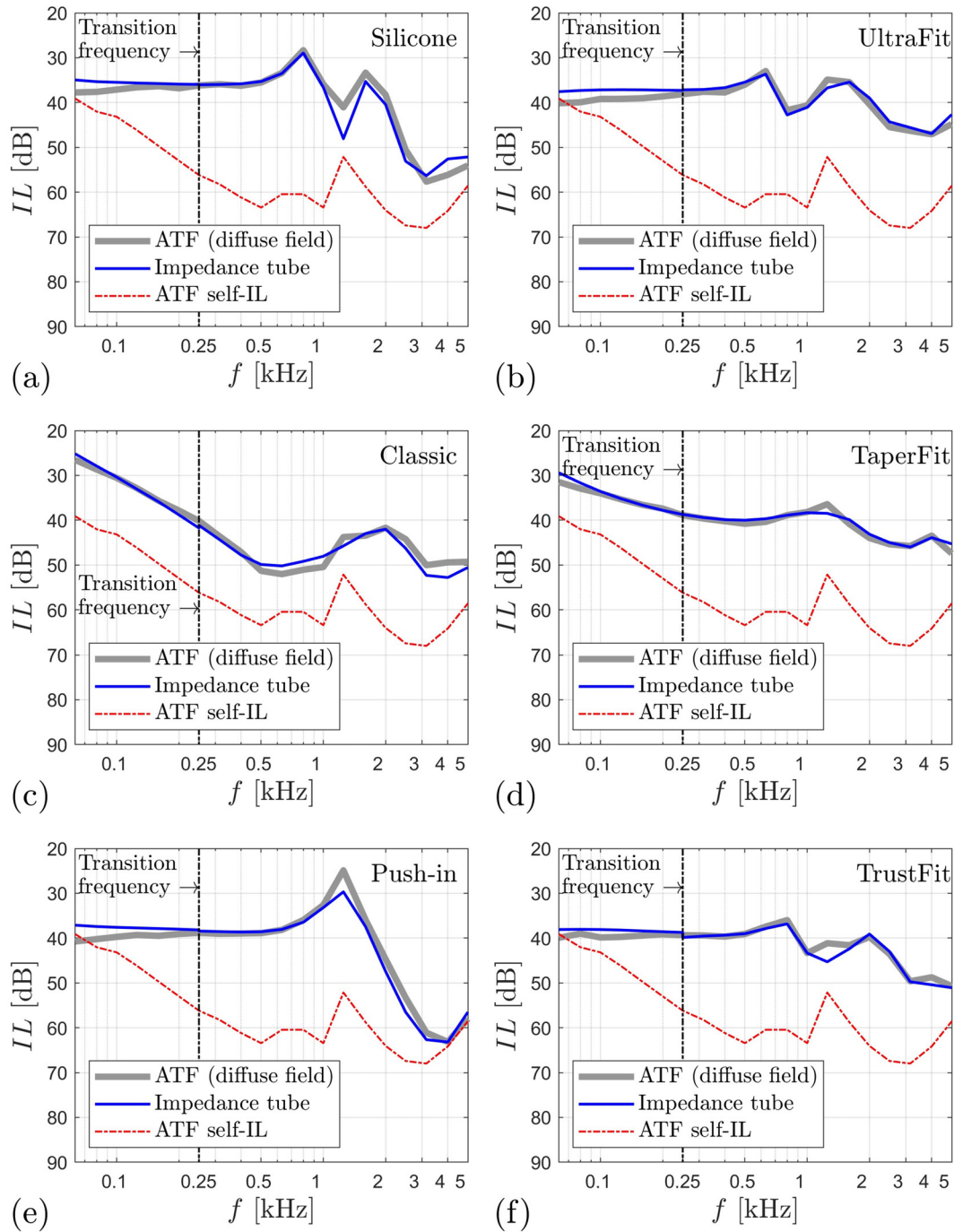
Carillo *et al.*   907

FIG. 5. (Color online) Third octave band IL measured on ATF and estimated using the proposed impedance tube method for the six tested earplugs from 63 Hz to 5 kHz. The self-IL of the ATF is also displayed.

The term TL_{EP} corresponds to the acoustic transmission loss of the earplug [refer to Eq. (5)], whereas the term IL_c is influenced by the reflection coefficient of the earplug's medial surface and the geometrical and acoustical properties of the earcanal [refer to Eq. (6)]. To exemplify this decomposition, Fig. 7 displays the IL of the homemade silicone earplug measured on the ATF and estimated using the impedance tube method, along with its decomposed terms TL_{EP} and IL_c. Results are presented in narrowband from 50 Hz to 6.5 kHz.

Given a specific earcanal geometry and acoustical properties, the IL decomposition enables the differentiation between the influence of the earplug's transmission loss and the influence of the reflection coefficient of its medial surface. According to Fig. 7, below 1 kHz, the earplug IL is adversely affected (decreased by $-20\,\mathrm{dB}$ at $100\,\mathrm{Hz}$) by acoustic reflections occurring at the earplug's medial surface, which acts as an acoustically rigid surface akin to conventional earplugs. If necessary, a method to enhance the low-frequency sound attenuation of earplugs is to design
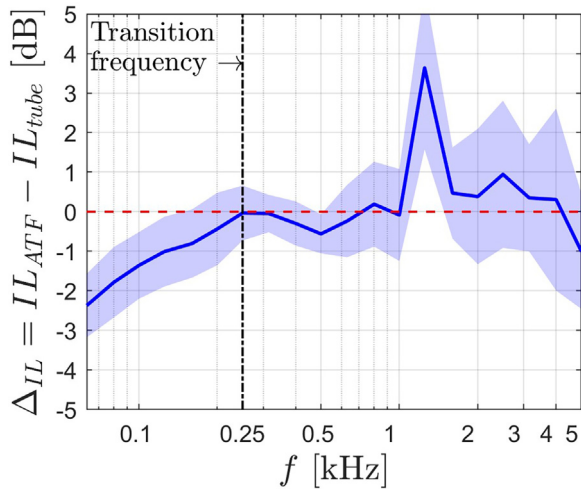
908   J. Acoust. Soc. Am. **156** (2), August 2024

Carillo *et al.*

FIG. 6. (Color online) Difference (mean ± standard deviation) between the third octave band IL measured on ATF and estimated using the proposed impedance tube method for the six tested earplugs.

FIG. 8. (Color online) Influence of the cross-section area of the impedance tube downstream section on the IL estimated using the impedance tube method.

them with a medial surface featuring low acoustic impedance, as developed in passive meta-earplugs addressing the occlusion effect using Helmholtz resonators,[22,23] such that IL_c would be close to zero and the earplug IL would rely exclusively on TL_{EP}. Conversely, around 3 kHz, the acoustically rigid medial surface of the earplug significantly increases (by almost 15 dB) the IL because it eliminates the quarter-wavelength acoustic resonance that occurs when the earcanal is open. This consideration is crucial in the design of flat/uniform attenuation earplugs.

As detailed in Sec. II B, the impedance tube setup that we used in this work incorporates a downstream section with a diameter identical to that of the ATF earcanal rather than the larger diameter of the impedance tube. This modification, aimed at enhancing the signal-to-noise ratio at microphone #3, is further analyzed here to assess its influence on the estimated IL. For this purpose, Fig. 8 displays

the estimated IL of the homemade silicone earplug for the small and "large" downstream cross sections. According to Fig. 8, we can see that the IL estimated using the large downstream section significantly differs from the IL estimated using the small downstream section. The discrepancies arise from the fact that the signal measured at microphone #3 is drowned in the background noise in the case of the large downstream section. This comes from the acoustic pressure drop that occurs in the large downstream section due to the change in section between the small cross section of the sample holder and large cross section of the impedance tube downstream section. The use of small downstream cross sections, which are not yet integrated into commercial impedance tubes, is crucial to ensure the proper functioning of the proposed impedance tube technique for estimating the earplug IL.

IV. CONCLUSION

In this paper, we conducted a comprehensive evaluation, numerically and experimentally, of a modified impedance tube technique designed for estimating the IL of earplugs measured on an ATF. The method involves assessing the acoustic properties of the earplugs, specifically the transmission loss and reflection coefficient of its medial surface, in a commercial impedance tube. These properties are then incorporated into a 1D analytical model of the earcanal. The numerical evaluation demonstrated the validity of the theoretical approach, even for long earplugs protruding outside the earcanal and excited by a diffuse sound field. The experimental evaluation included six earplugs, representing various earplug families. The experimental results showed that the modified impedance tube method provides accurate estimates of the IL measured on the ATF. This achievement was made possible by modifying the impedance tube setup, specifically by reducing the diameter of the tube's downstream section, which significantly improved the signal-to-noise ratio at microphone #3. Additionally, the method
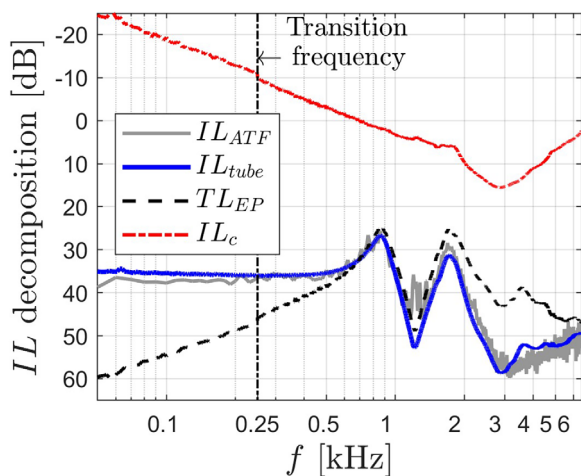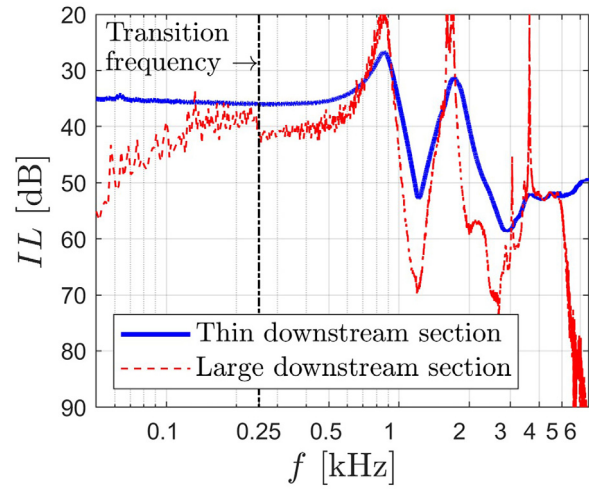

FIG. 7. (Color online) Narrowband IL measured on ATF and estimated using the impedance tube method for the homemade silicone earplug from 50 Hz to 6.5 kHz. Decomposition terms, TL_{EP} and IL_c, of the impedance tube IL are also displayed.

demonstrated its utility in straightforwardly decomposing the IL to study the influence of the earplug's acoustic properties on the phenomenon. Therefore, the impedance tube method emerges as a practical tool for IL assessment, particularly during the development phase of earplugs aiming for specific vibro-acoustic responses, such as flat sound attenuation. Compared to ATF setup, the impedance tube method eliminates the need for a cumbersome acoustic room and does not suffer from bone-conduction limit. This method could also be used for measuring earplug IL at high SPL with precise control of the excitation amplitude. Furthermore, the impedance tube method enables the incorporation of (i) human earcanal geometry variability by using different sample holders, and (ii) the variability of the eardrum impedance directly in the post-processing. Yet, compared to the ATF method, the impedance tube method is limited in frequency, reaching a maximum working frequency corresponding to the cut-off frequency of the 29 mm diameter impedance tube used in this study, approximately 6.5 kHz. Also, it is important to note that our ATF setup was simplified, and certain factors, such as the pinna and the heating system, were not considered yet. These limitations will be addressed in future work, involving adaptations to the classical impedance tube setup to include these factors.

ACKNOWLEDGMENTS

AUTHOR DECLARATIONS
Conflict of Interest

The authors have no conflicts to declare.

DATA AVAILABILITY

The data that support the findings of this study are available from the corresponding author upon reasonable request.

APPENDIX A: RADIATION ACOUSTIC IMPEDANCE

The specific radiation acoustic impedance, Z_R, defined at the earcanal opening is equal to that of a baffled circular piston of radius r_{EC}, coupled to a semi-infinite acoustic domain, and is given by[12]

$$Z_R = \rho_0 c_0 \left(1 - \frac{J_1(2k_0 r_{EC})}{k_0 r_{EC}} + j \frac{H_1(2k_0 r_{EC})}{k_0 r_{EC}} \right), \qquad \text{(A1)}$$

where J_1 and H_1 are the first order Bessel and Struve functions, respectively, and $k_0 = \omega/c_0$ is the lossless wavenumber, ρ_0 is the air density, and c_0 is the sound speed in air.

APPENDIX B: LOW REDUCED FREQUENCY MODEL

The low reduced frequency model[11] is used to account for viscous and thermal losses that exist in cylindrical tubes (e.g., earcanal and impedance tube) of radius r_i and is valid when the acoustic wavelength is much larger than the tube cross section and boundary layer thickness. In this model, the equivalent wavenumber, k_{eq}^i, and the equivalent characteristic impedance, Z_{eq}^i, are given by

$$k_{eq}^i = k_0 \left[\frac{\gamma - (\gamma - 1)\psi_{th}}{\psi_{vi}} \right]^{1/2}, \qquad \text{(B1)}$$

$$Z_{eq}^i = Z_0 [\psi_{vi}(\gamma - (\gamma - 1)\psi_{th})]^{-1/2}, \qquad \text{(B2)}$$

where γ corresponds to the ratio of specific heats, and ψ_{vi} and ψ_{th} correspond to geometry- and material-dependent functions, respectively, associated with viscous and thermal effects and defined by
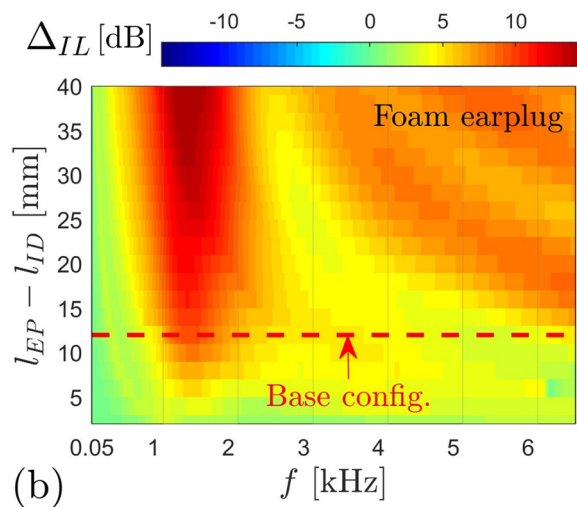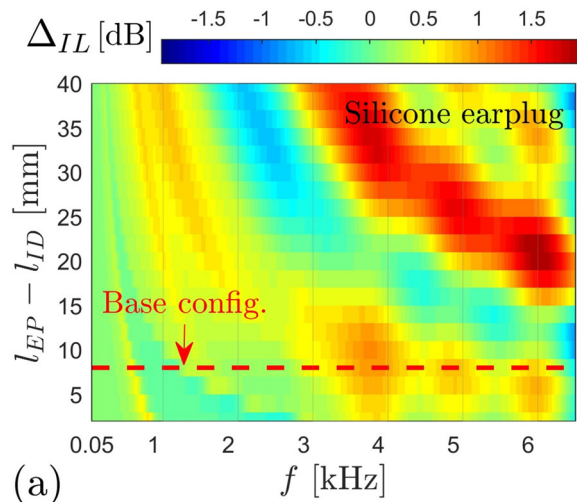

FIG. 9. (Color online) Frequency-dependent differences (ΔIL) in IL between the impedance tube method and ATF under normal incidence plane wave excitation as a function of the protrusion length ($l_{EP} - l_{ID}$) for (a) silicone and (b) foam earplugs are shown. The IL calculated using the impedance tube method assumes that $S_{eff} = S_{EC}$, thereby disregarding the protrusion effect.

$$\psi_{vi} = -\frac{J_2(k_{vi}r_i)}{J_0(k_{vi}r_i)}, \tag{B3}$$

$$\psi_{th} = -\frac{J_2(k_{th}r_i)}{J_0(k_{th}r_i)}, \tag{B4}$$

where J_α is the first order Bessel function of integer order α, $k_{vi} = \sqrt{-j\omega\rho_0/\mu}$ and $k_{th} = \sqrt{-j\omega\rho_0 C_p/\kappa}$ are the viscous and thermal wavenumbers, respectively, while μ, C_p, and κ represent, respectively, the dynamic viscosity, heat capacity at constant pressure, and thermal conductivity coefficient.

APPENDIX C: INFLUENCE OF NEGLECTING EARPLUG PROTRUSION IN THE IMPEDANCE TUBE METHOD

Figures 9(a) and 9(b) show the frequency-dependent difference (ΔIL) in IL between the impedance tube and ATF (normal incidence plane wave excitation).

[1]ANSI/ASA S12.42-2010: *Methods for the Measurement of Insertion Loss of Hearing Protection Devices in Continuous or Impulsive Noise Using Microphone-in-Real-Ear or Acoustic Test Fixture Procedures* (Acoustical Society of America, New York, 2010).

[2]B. Poissenot-Arrigoni, C. H. Law, D. Berbiche, F. Sgard, and O. Doutres, "Morphologic clustering of earcanals using deep learning algorithm to design artificial ears dedicated to earplug attenuation measurement," J. Acoust. Soc. Am. **152**, 3155–3169 (2022).

[3]P. Hiselius, "Method to assess acoustical two-port properties of earplugs," Acta Acust. Acust. **90**, 137–151 (2004).

[4]P. Hiselius, "Attenuation of earplugs—Objective predictions compared to subjective REAT measurements," Acta Acust. Acust. **91**, 764–770 (2005).

[5]O. Doutres, F. Sgard, and G. Viallet, "Measurement of earplugs insertion loss using a classical impedance tube," in *the 44th International Congress and Exposition on Noise Control Engineering*, San Francisco, CA (August 9–12) (INCE-USA, Wakefield, MA, 2015), pp. 4114–4124, available at https://espace2.etsmtl.ca/id/eprint/11322/ (Last viewed 2 August 2024).

[6]ASTM E2611-09, "Standard test method for measurement of normal incidence sound transmission of acoustical materials based on the transfer matrix method," (American Society for Testing and Materials, New York, 2009), available at https://www.astm.org/e2611-09.html (Last viewed 20 July 2023).

[7]K. Carillo, O. Doutres, and F. Sgard, "Experimental validation of an impedance tube measurement method for assessing earplugs insertion loss," available at https://espace2.etsmtl.ca/id/eprint/17463/ (Last viewed 2 August 2024).

[8]Y. Salissou, R. Panneton, and O. Doutres, "Complement to standard method for measuring normal incidence sound transmission loss with three microphones," J. Acoust. Soc. Am. **131**, EL216–EL222 (2012).

[9]G. Viallet, F. Sgard, F. Laville, and J. Boutin, "A finite element model to predict the sound attenuation of earplugs in an acoustical test fixture," J. Acoust. Soc. Am. **136**, 1269–1280 (2014).

[10]E. H. Berger, R. W. Kieper, and M. E. Stergar, "Performance of new acoustical test fixtures complying with ANSI S12.42-2010, with particular attention to the specification of self insertion loss," in *Internoise 2012*, New York (19–22 August 2012) (Institute of Noise Control Engineering, Wakefield, MA, 2012), pp. 517–528.

[11]W. R. Kampinga, "Viscothermal acoustics using finite elements: Analysis tools for engineers," Ph.D. thesis, University of Twente, Enschede, 2010.

[12]M. Bruneau, *Fundamentals of Acoustics* (Wiley, New York, 2013).

[13]K. M. Ho, Z. Yang, X. X. Zhang, and P. Sheng, "Measurements of sound transmission through panels of locally resonant materials between impedance tubes," Appl. Acoust. **66**, 751–765 (2005).

[14]E. H. Berger, "Methods of measuring the attenuation of hearing protection devices," J. Acoust. Soc. Am. **79**, 1655–1687 (1986).

[15]ANSI/ASA S3.25-2009 (R2014): *Occluded Ear Simulator* (Acoustical Society of America, New York, 2014), available at https://webstore.ansi.org/standards/asa/ansiasas3252009r2014 (Last viewed 17 December 23).

[16]F. Q. Hu, "On absorbing boundary conditions for linearized Euler equations by a perfectly matched layer," J. Comput. Phys. **129**, 201–219 (1996).

[17]Y. Luan, F. Sgard, H. Nélisse, and O. Doutres, "A finite element model to predict the double hearing protector effect on an in-house acoustic test fixture," J. Acoust. Soc. Am. **151**, 1860–1874 (2022).

[18]F. C. Sgard, N. Atalla, and J. Nicolas, "A numerical model for the low frequency diffuse field sound transmission loss of double-wall sound barriers with elastic porous linings," J. Acoust. Soc. Am. **108**, 2865–2872 (2000).

[19]N. Atalla and F. Sgard, *Finite Element and Boundary Methods in Structural Acoustics and Vibration* (CRC Press, Boca Raton, 2015).

[20]K. Carillo, O. Doutres, and F. Sgard, "Numerical investigation of the earplug contribution to the low-frequency objective occlusion effect induced by bone-conducted stimulation," J. Acoust. Soc. Am. **150**, 2006–2023 (2021).

[21]ANSI/ASA S1.11-2004 (R2009): *Octave-Band and Fractional-Octave-Band Analog and Digital Filters* (Acoustical Society of America, New York, 2009), available at https://webstore.ansi.org/standards/asa/ansiasas1112004r2009 (Last viewed 13 December 23).

[22]K. Carillo, F. Sgard, O. Dazel, and O. Doutres, "Reduction of the occlusion effect induced by earplugs using quasi perfect broadband absorption," Sci. Rep. **12**, 15336 (2022).

[23]K. Carillo, F. Sgard, O. Dazel, and O. Doutres, "Passive earplug including Helmholtz resonators arranged in series to achieve broadband near zero occlusion effect at low frequencies," J. Acoust. Soc. Am. **154**, 2099–2111 (2023).